Review

Accelerated Burn Healing in a Mouse Experimental Model by α-gal Nanoparticles

Uri Galili *

Posted Date: 6 September 2023

doi: 10.20944/preprints202309.0375.v1

Keywords: Burn healing; anti-Gal antibody; α-gal epitope; α-gal nanoparticles; macrophage migration; α-gal therapy; mesenchymal stem cells.

Review

Accelerated Burn Healing in a Mouse Experimental Model by α-gal Nanoparticles

Uri Galili

Department of Medicine, Rush University Medical College, Chicago, IL 60612, USA; uri.galili@rcn.com; Tel.: +001-312-753-5997

Abstract: Macrophages play a pivotal role in the process of healing burns. One of the major risks in the course of burns healing, in the absence of regenerating epidermis, is infections which greatly contribute to morbidity and mortality in such patients. Therefore, it is widely agreed that accelerating recruitment of macrophages into burns may contribute to faster regeneration of the epidermis and thus, decreasing the risk of infections. This review describes a unique method for rapid recruitment of macrophages into burns and activation of these macrophages to mediate accelerated regrowth of the epidermis and healing of burns. The method is based on application of bio-degradable "α-gal" nanoparticles to burns. These nanoparticles present multiple α-gal epitopes (Gal 1-3Gal 1-4GlcNAc-R) which bind the abundant natural anti-Gal antibody that constitutes ~1% of immunoglobulins in humans. Anti-Gal/α-gal nanoparticles interaction activates the complement system, resulting in localized production of the complement cleavage-peptides C5a and C3a that are highly effective chemotactic factors for monocytes derived macrophages. The macrophages recruited into the α-gal nanoparticles treated burns are activated following interaction between the Fc portion of anti-Gal coating the nanoparticles and the multiple Fc receptors on macrophages cell membranes. The activated macrophages secrete a variety of cytokines/growth factors that accelerate the regrowth of the epidermis and regeneration of the injured skin, thereby cutting the healing time by half. Studies on healing of thermal injuries in the skin of anti-Gal producing mice, demonstrated a much faster recruitment of macrophages into burns treated with α-gal nanoparticles than in control burns treated with saline and healing of the burns within 6 days, whereas healing of control burns takes ~12 days. α-Gal nanoparticles are non-toxic, and do not cause chronic granulomas or keloids. These findings suggest that α-gal nanoparticles treatment may harness anti-Gal for inducing similar accelerated burn healing effects also in humans.

Keywords: burn healing; anti-Gal antibody; α-gal epitope; α-gal nanoparticles; macrophage migration; α-gal therapy; mesenchymal stem cells

1. Introduction

Macrophages play a pivotal role in the process of wound and burn healing [1–4]. In both types of healing the M1 macrophages first debride the injured skin of apoptotic and dead cells and of intercellular cell matrix. Subsequently, M2 macrophages orchestrate the regeneration of the epidermis, dermis and hypodermis of the injured skin [2–6]. This is mediated by a wide range of cytokines/growth factors secreted by these macrophages, including vascular endothelial growth factor (VEGF) mediating neo-vascularization, epidermal growth factor (EGF) inducing epidermal re-growth, fibroblasts growth factor (FGF) recruiting fibroblasts, and factors recruiting mesenchymal stem cells (MSC) which contribute to the regeneration of the injured skin [7]. In wounds, incisions, and contusions, the macrophages mediating healing comprise of both residential macrophages and monocytes derived macrophages that are recruited by chemotactic factors such as macrophage inflammatory protein-1 (MIP-1), monocyte chemoattractant protein-1 (MCP-1) and regulated on activation, normal T cell expressed and secreted factor (RANTES) secreted by cells surrounding the wound [8–11]. However, since in epidermis penetrating burns (burn degrees 2-4) the residential

 doi:10.20944/preprints202309.0375.v1

macrophages are inactivated or killed [1] and since the surface area size of the burns are in many cases larger than that of wounds, infiltration of macrophages into burns and healing of burns may take longer time than in wounds and regeneration of epidermis in many burns may be slower than in wounds. This slow re-epithelialization is a major risk factor because of microbial infections that occur in the absence of intact epidermis. Such infections may result in high morbidity and mortality following severe burn injuries [6,12–14].

Based on the pivotal role of macrophages in healing of burns, and in view of the immune suppression of macrophages following burn injury [15,16], it has been suggested that the risk factors due to slow re-epithelialization might be reduced by accelerating the regrowth of the epidermis over the burned tissue [3,4,7,15–18]. Several methods of various degrees of difficulty have been studied for accelerating burn healing. These include topical application to burns of autologous MSC [19,20], autologous cultured epidermal cell grafts [21,22], recombinant human granulocyte-macrophage colony-stimulating factor (GM-CSF) [23,24], high-density lipoprotein nanoparticles [25], bioactive molecules delivered in microfibers [26,27] and the use of negative pressure wound therapy[28].

The present review offers an alternative method to those mentioned above, for accelerated healing of burns by inducing rapid recruitment and activation of macrophages in treated burns, by topical application of a-gal nanoparticles. This method recapitulates the physiologic healing processes of burns, but the accelerated recruitment of macrophages into treated burns cuts the healing time by half. The interaction of these nanoparticles with the natural anti-Gal antibody (one of the most abundant natural antibodies in humans) within burns results in rapid and extensive recruitment of monocytes derived macrophages into burns. Many of these macrophages polarize into M2 macrophages which orchestrate accelerated healing of burns by localized secretion of angiogenic factors such as VEGF and growth factors recruiting MSC. This review describes studies that characterized the anti-Gal antibody and a-gal nanoparticles, the simple production of these nanoparticles from mammalian red blood cells and the great efficacy of the burn and wound therapies with a-gal nanoparticles, as observed in the anti-Gal producing mouse experimental model.

2. Anti-Gal and the a-gal Epitope

The method described in this review for accelerating burn healing harnesses the immunologic potential of the natural anti-Gal antibody which is one of the most abundant natural antibodies in humans, constituting 1% of serum immunoglobulins [29]. The immune system in humans produces anti-Gal throughout life in response to antigenic stimulation by some carbohydrate antigens presented on gastrointestinal bacteria [30,31]. The mammalian antigen recognized by the anti-Gal is the a-gal epitope (Gala1- 3Galb1-4GlcNAc-R) [32–34]. The a-gal epitope is abundantly expressed on glycolipids and glycoproteins of nonprimate mammals, lemurs, and New-World monkeys (monkeys of South America), therefore, these mammals cannot produce anti-Gal [35–37]. In contrast, humans, apes, and Old-World monkeys (monkeys of Asia and Africa) all lack a-gal epitopes but produce the natural anti-Gal antibody [35–38]. Incubation of cells presenting a-gal epitope in human serum results in effective activation of the complement cascade in the serum, because of the binding of serum anti-Gal to these a-gal epitopes. The efficacy of this complement activation was demonstrated in xenotransplantation studies. Interaction between anti-Gal and a-gal epitopes on endothelial cells of pig xenografts was found to result in the activation of the complement system, causing cytolysis of these cells, collapse of the vascular bed and rapid (hyperacute) rejection of such xenografts in monkeys or humans [39–42]. Similarly, incubation of enveloped viruses presenting a-gal epitopes in human serum was found to result in binding of anti-Gal to these epitopes and in activation of the complement system which leads to complement mediated destruction of such viruses [43–46]. Since the very potent macrophage directing chemotactic factors C5a and C3a are produced as complement cleavage peptide byproducts during complement activation, we assumed that binding of serum anti-Gal to multiple a-gal epitopes on a-gal nanoparticles applied to burns and wounds may result in extensive recruitment of monocyte derived macrophages to treated skin injury sites.

3. Hypothesis

Preprints (www.preprints.org) | NOT PEER-REVIEWED | Posted: 6 September 2023 doi:10.20944/preprints202309.0375.v1

The effective complement activation by anti-Gal binding to a-gal epitopes led us to hypothesize that topical application of nanoparticles presenting multiple a-gal epitopes (called a-gal nanoparticles and previously called a-gal liposomes) during the early stages of hemostasis in burns, results in binding of the natural anti-Gal antibody to these nanoparticles [17,47]. Anti-Gal is present in the fluid film on the surface of burns together with the complement system proteins, as well as with other serum proteins which leak from injured capillaries. As detailed below, a-gal nanoparticles are small size liposomes (~200-300 nm) constructed of a-gal presenting glycolipids that are anchored in the nanoparticles wall that is comprised of phospholipids and cholesterol (Figure 1A).

The binding of anti-Gal to the multiple a-gal epitopes on the nanoparticles results in activation of the complement cascade and thus in generation of chemotactic complement cleavage peptides C5a and C3a (Step 1 in Figure 1B). These chemotactic factors induce extensive migration of neutrophils and monocytes derived macrophages into the burn area (Step 2 in Figure 1B). In addition, it was further hypothesized that whereas the neutrophils survive only for few hours in the burn, the recruited macrophages are long-lived, and they bind the a-gal nanoparticles as a result of interaction between the Fcg "tail" of anti-Gal bound to the nanoparticles and Fcg receptors (FcgR) on the macrophages (Step 3 in Figure 1B). It was further hypothesized that the multiple Fcg/FcgR interactions between anti-Gal coated a-gal nanoparticles and macrophages may activate the recruited macrophages to secrete various cytokines/growth factors that mediate accelerated migration of fibroblasts and MSC into the treated burn, as well as neo-vascularization of the healing burn (Step 4 in Figure 1B), and rapid re-epithelialization. Ultimately, these multiple cytokines/growth factors secreted by the recruited and activated macrophages may accelerated healing of the a-gal nanoparticles treated burns in comparison to non-treated burns.

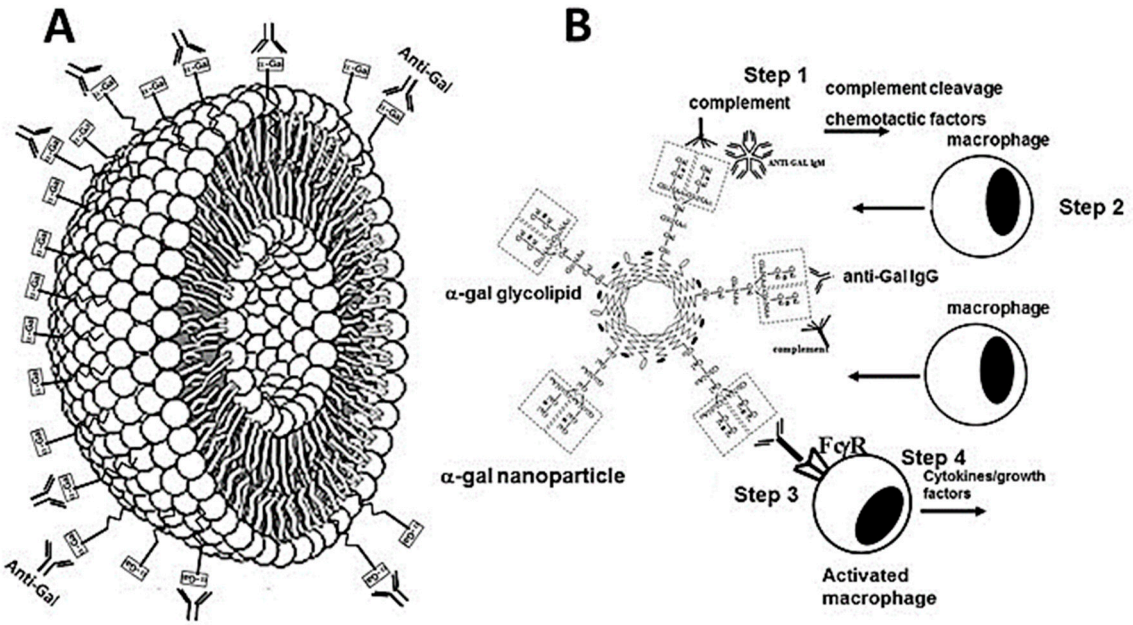

Figure 1. Illustration of an α-gal nanoparticle (A) and hypothesized immune processes induced by α-gal nanoparticles applied to burns (B). A. The α-gal nanoparticles present multiple α-gal epitopes (rectangles) on glycolipids that are anchored in the phospholipid bilayer that forms the wall of the nanoparticle. The nanoparticle wall may also contain cholesterol which stabilizes the wall. The natural anti-Gal antibody readily binds to these α-gal epitopes (illustrated as rectangles). B. The steps hypothesized to occur in burns after application of α-gal nanoparticles: Step 1- Anti-Gal binding to α-gal nanoparticles activates the complement system. Step 2- The complement cleavage peptides C5a and C3a formed as a result of complement activation, function as chemotactic factors that direct extensive and rapid recruitment of monocytes derived macrophages into the treated burns. Step 3- The recruited macrophages interact via their Fcγ receptors (FcγR) with the Fcγ portion (tail) of anti-Gal coating the α-gal nanoparticles. Step 4- The Fcγ/FcγR interactions activate the macrophages to

 doi:10.20944/preprints202309.0375.v1

secrete cytokines/growth factors that induce accelerated healing of the treated burns. Reproduced from ref. 47 with permission.

4. Preparation of a-gal Nanoparticles

A relatively simple way for preparing a-gal nanoparticles is by extraction of their components from the membranes (ghosts) of rabbit red blood cells (RBC) in a mixture of chloroform and methanol [17]. The reason for using these RBC is that they present as many as $2x10^6$ a-gal epitopes per RBC, an amount that is several folds higher than any other mammalian RBC studied [35]. After the rabbit RBC are lysed in water and their membranes are washed for the removal of hemoglobin, the RBC membranes are incubated overnight in a solution of chloroform:methanol 1:2 with constant stirring, resulting in the extraction of phospholipids, glycolipids and cholesterol from these membranes, whereas all proteins are denatured and removed from the solution by filtration. The solution containing the extracted molecules is dried and the mixture of phospholipids, glycolipids and cholesterol is resuspended in saline by extensive sonication. This sonication results in formation of a suspension of submicroscopic liposomes (~100-300 nm) with walls comprised of phospholipid and cholesterol and studded with multiple a-gal epitopes in the form of anchored a-gal glycolipids (Figures 1A). These submicroscopic liposomes originally called a-gal liposomes [17,48] have been subsequently referred to as a-gal nanoparticles [18,47] to indicate that they do not contain any substance in their lumen.

The a-gal nanoparticles were found to present ~10^{14} a-gal epitopes/mg nanoparticles [18]. Processed 500 ml packed rabbit RBC were found to yield ~6 grams of a-gal nanoparticles. Because of their small size, a-gal nanoparticles suspensions can be sterilized by filtration through a 0.4 mm filter. It is of note that a-gal nanoparticles may be prepared also from synthetic a-gal glycolipids, phospholipids and cholesterol by similar mixing and sonication processes. The a-gal nanoparticles are highly stable and can be kept as frozen suspensions for >10 years, at 4^oC for >2 years and as dried nanoparticles on wound dressings kept at room temp. for >1 year (unpublished observations). Stability of the stored a-gal nanoparticles could be confirmed by their ability to bind anti-Gal in amounts like those measured immediately after production. Topical application of a-gal nanoparticles to burns and wounds can be performed by various methods including the use of nanoparticles suspensions in saline or PBS, nanoparticles dried on wound dressings, aerosol suspensions and suspensions in hydrogels.

5. Experimental Animal Models

Studies of anti-Gal associated therapies cannot be performed in standard animal experimental models such as mice, rats, rabbits, pigs or guinea pigs because these animals, like other non-primate mammals, synthesize a-gal epitopes [35,36]. Therefore, such mammals are immunotolerant to the a-gal epitope and cannot produce the anti-Gal antibody [35]. However, the two experimental non-primate mammalian models available for studying anti-Gal associated therapies have been mice [49,50] and pigs [51,52] in which the *GGTA1* gene coding for the glycosyltransferase synthesizing a-gal epitope "a1,3galactosyltransferase", was disrupted (i.e., knocked out). These a1,3galactosyltransferase knockout (GT-KO) mice [17,18] and pigs [53–55] lack the ability to synthesize a-gal epitopes and thus, can produce the anti-Gal antibody. Whereas GT-KO pigs produce the natural anti-Gal antibody, as humans do, GT-KO mice do not naturally produce this antibody since they do not develop gastrointestinal bacterial flora that may immunize them, because they are kept in a sterile environment and receive sterile food. Nevertheless, GT-KO mice readily produce the anti-Gal antibody following several immunizations with xenogeneic cells or tissues presenting a-gal epitopes, such as pig kidney membranes (PKM) homogenate [56].

6. *In vitro* Effects of a-gal Nanoparticles on Macrophages

Some of the steps of anti-Gal/a-gal nanoparticles interaction, described in the hypothesis illustrated in Figure 1B, could be demonstrated *in vitro* in studies described in Figure 2. Step 1 of anti-Gal binding to a-gal epitopes on a-gal nanoparticles was demonstrated by the specific binding of

Preprints (www.preprints.org) | NOT PEER-REVIEWED | Posted: 6 September 2023 doi:10.20944/preprints202309.0375.v1

monoclonal anti-Gal antibody to these nanoparticles (Figure 2A). A similar binding was observed with serum anti-Gal from anti-Gal producing GT-KO mice that interacts woth a-gal nanoparticles (Figure 2B). In the absence of a-gal epitopes on the nanoparticles, no binding of the monoclonal anti-Gal antibody was observed [17].

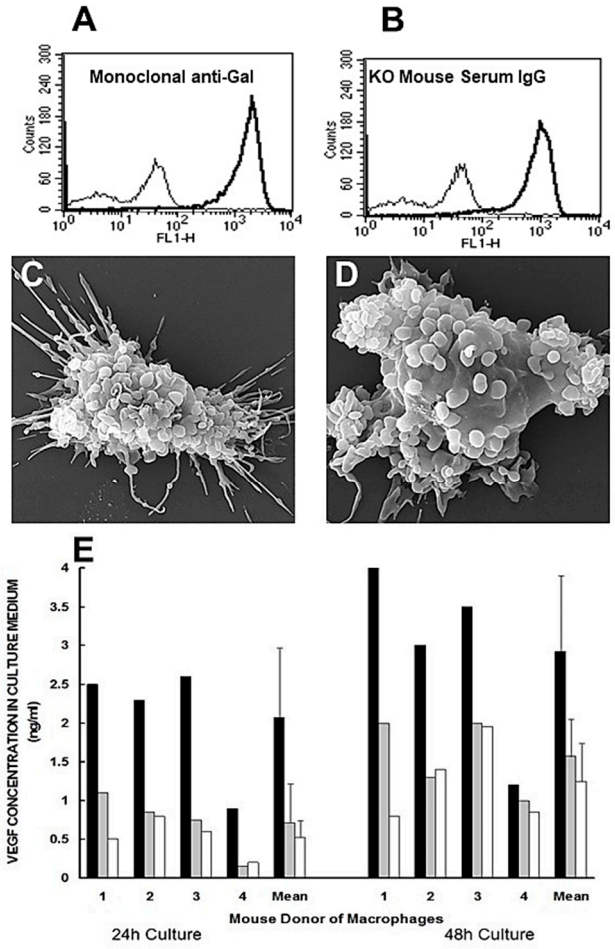

Figure 2. *In vitro* demonstration of anti-Gal binding to α-gal nanoparticles and the resulting effects on macrophages. A. Binding of monoclonal anti-Gal IgM antibody to α-gal epitopes on α-gal nanoparticles. The thin line represents the IgM isotype control. B. As in Figure 2A, using anti-Gal IgG in serum of α1,3galactosyltransferase knockout (GT-KO) mouse producing anti-Gal. The thin line represents the IgG isotype control. C and D. Binding of anti-Gal-coated α-gal nanoparticles to adherent GT-KO pig macrophages as shown by scanning electron microscopy (SEM), after 2 hours incubation of anti-Gal coated nanoparticles with the macrophages at room temp., followed by washings to remove nonadherent nanoparticles. The surfaces of representative macrophages are covered with α-gal nanoparticles that have the shape of small spheres. The size of the α-gal nanoparticles is ~100-300 nm. E. GT-KO mouse peritoneal macrophages secretion of VEGF following incubation with anti-Gal-coated α-gal nanoparticles (closed columns), α-gal nanoparticles without anti-Gal (grey columns), or as macrophages alone (open columns, background levels). VEGF secretion by the macrophages was measured by ELISA in culture media after 24 or 48 hours. Data with macrophages from 4 GT-KO mice and their means+S.D. Modified from ref. 47 with permission.

Step 3 in the hypothesis in Figure 1B predicts binding of anti-Gal coated α-gal nanoparticles to macrophages via Fcg/FcgR interaction. This binding is demonstrated by scanning electron microscopy (SEM) in Figure 2C,D. Macrphages lacking a-gal epitopes were generated *in vitro* by culturing of monocytes obtained from blood of GT-KO pigs. These macrophages were co-incubated for 2 hours at room temp. with anti-Gal-coated α-gal nanoparticles. Such incubation resulted in extensive binding of α-gal nanoparticles to the macrophages, shown as the multiple small spheres

 doi:10.20944/preprints202309.0375.v1

(size of 100–300nm) covering the surface of the two macrophages (Figure 2C,D). In the absence of anti-Gal on the α-gal nanoparticles, no binding of these nanoparticles to macrophages was observed [47]. Step 4 in the hypothesis in Figure 1B predicted that the binding of anti-Gal coated a-gal nanoparticles to recruited macrophages via Fcγ/FcγR interaction may generate signals that activate a variety of cytokines/growth factors producing genes that orchestrate accelerated healing of a-gal nanoparticles treated burns. Possible activation of macrophages by anti-Gal coated a-gal nanoparticles was studied with GT-KO mouse macrophages incubated for 24-48 hours at 37°C, alone or with α-gal nanoparticles coated with anti-Gal or lacking the antibody. The secretion of VEGF by the macrophages was measured in the tissue culture medium after 24 and 48 hours of co-incubation. Macrophages co-incubated with α-gal nanoparticles lacking anti-Gal, secreted only background level of VEGF, as determined by ELISA measuring this cytokine (Figure 2E). However, co-incubation of the macrophages with anti-Gal-coated α-gal nanoparticles for 24 and 48 hours resulted in elevated secretion of VEGF by the activated macrophages, at levels that were significantly higher than the background levels (Figure 2E) [48]. These findings indicated that anti-Gal mediated binding of a-gal nanoparticles to cultured macrophages indeed induces these macrophages to secrete VEGF.

7. *In vivo* Effects of a-gal Nanoparticles on Macrophages

A crucial step in the hypothesis in Figure 1B is Step 2 which predicts that anti-Gal binding to a-gal nanoparticles applied to burns activates the complement system, resulting in the formation of complement cleavage chemotactic peptides C5a and C3a. These peptides direct a rapid and extensive recruitment of monocytes derived macrophages to the treated burn. The occurrence of Step 2 was studied by intradermal injection of 10 mg a-gal nanoparticles in anti-Gal producing GT-KO mice (i.e., GT-KO mice immunized with PKM) and microscopic evaluation of macrophages in the injection site at various time points. The first effect of such injection was the accumulation of many neutrophils, observed at the injection site within 12 hours post injection [48]. These neutrophils are also chemotactically recruited by C5a and C3a generated by anti-Gal/a-gal nanoparticles interaction. However, after 24 hours, most neutrophils disappeared, and multiple mononuclear cells were observed migrating to the injection site (Figure 3A). The number of macrophages increased after 4 days and as expected, they all were immunostained by the macrophage specific antibody F4/80 (Figure 3B). Quantitative real time PCR (qRT-PCR) of skin specimen containing the recruited macrophages displayed activation of genes encoding for fibroblast growth factor (FGF), interleukin 1 (IL1), platelet derived growth factor (PDGF), and colony stimulating factor (CSF) [48].

The number of recruited macrophages further increased by Day 7 (Figure 3C). These macrophages had large size and ample cytoplasm, characteristic of activated macrophages (Figure 3C,D) [48]. Large numbers of recruited macrophages were observed at the injection site, even on Day 14. However, by Day 21 post injection of the a-gal nanoparticles, all macrophages disappeared from the injection site and the skin in that area displayed normal structure with no granuloma, chronic inflammatory response, or keloid formation [48]. Intradermal injection of a-gal nanoparticles together with cobra venom factor (a complement activation inhibitor), with saline, or with nanoparticles lacking a-gal epitopes (i.e., nanoparticles produced from GT-KO pig RBC) all resulted in no significant recruitment of macrophages to the injection site [48]. Similarly, intradermal injection of a-gal nanoparticles into wild-type (WT) mice (i.e., mice lacking the anti-Gal antibody) resulted in no macrophage recruitment. These observations clearly demonstrated the ability of a-gal nanoparticles to induce extensive and rapid recruitment of macrophages by binding of the anti-Gal antibody and activation of the complement system which generates the potent chemotactic complement cleavage chemotactic peptides C5a and C3a.

Preprints (www.preprints.org) | NOT PEER-REVIEWED | Posted: 6 September 2023 doi:10.20944/preprints202309.0375.v1

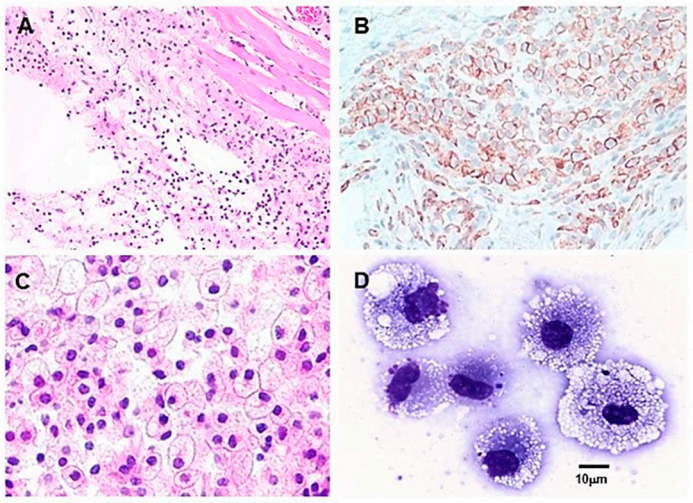

Figure 3. Macrophages recruitment by intradermally injected α-gal nanoparticles (10 mg), in anti-Gal producing GT-KO mice. A. Macrophage recruitment 24 hours following injection of α-gal nanoparticles. The empty oval area is the space formed by the injection of α-gal nanoparticles. The nanoparticles were dissolved by alcohol during staining with hematoxylin & eosin staining (H&E ×100). B. Macrophages at 4 days post injection, identified by immunostaining with the F4/80 antibody coupled to peroxidase (HRP) (×200). C. The injection area after 7 days. The site is full of many large macrophages containing vacuoles with morphology characteristic of activated macrophages (H&E × 400). D. Individual macrophages, similar to those in (C) were harvested from polyvinyl alcohol (PVA) sponge disc containing α-gal nanoparticles. The PVA sponge discs were explanted 6 days post subcutaneous implantation into anti-Gal producing GT-KO mice. The multiple vacuoles observed in the macrophages are of internalized anti-Gal coated α-gal nanoparticles (Wright staining, ×1000). Modified from ref. 47 with permission.

8. Macrophages Recruited by a-gal Nanoparticles are M2 Further Recruiting MSC

Analysis of the characteristics of macrophages recruited by a-gal nanoparticles in anti-Gal producing GT-KO mice could be further performed by subcutaneous implantation of biologically inert sponge discs (made of polyvinyl alcohol- PVA, 10 mm diameter, 3 mm thickness) that contained 10 mg α-gal nanoparticles. The PVA sponge discs were explanted on Day 6 or Day 9. The cells harvested from these sponge discs had the morphology of large macrophages as those presented in Figure 3D. Each of the PVA sponge discs contained at those time points ~$0.4x10^6$ and ~$0.6x10^6$ infiltrating cells, respectively, whereas sponge discs with only saline contained ~$0.02x10^6$ and ~$0.04x10^6$ cells, respectively [17]. Immunostaining and flow cytometry analysis of the cells recruited by a-gal nanoparticles indicated that most of them (>90%) expressed the macrophage markers CD11b and CD14 (Figure 4A). In contrast, no significant proportion of the infiltrating cells displayed surface markers of CD4+ T cells, CD8+ T cells, or of B cells (i.e., lymphocytes presenting CD20+ cell marker) [17].

Preprints (www.preprints.org) | NOT PEER-REVIEWED | Posted: 6 September 2023 doi:10.20944/preprints202309.0375.v1

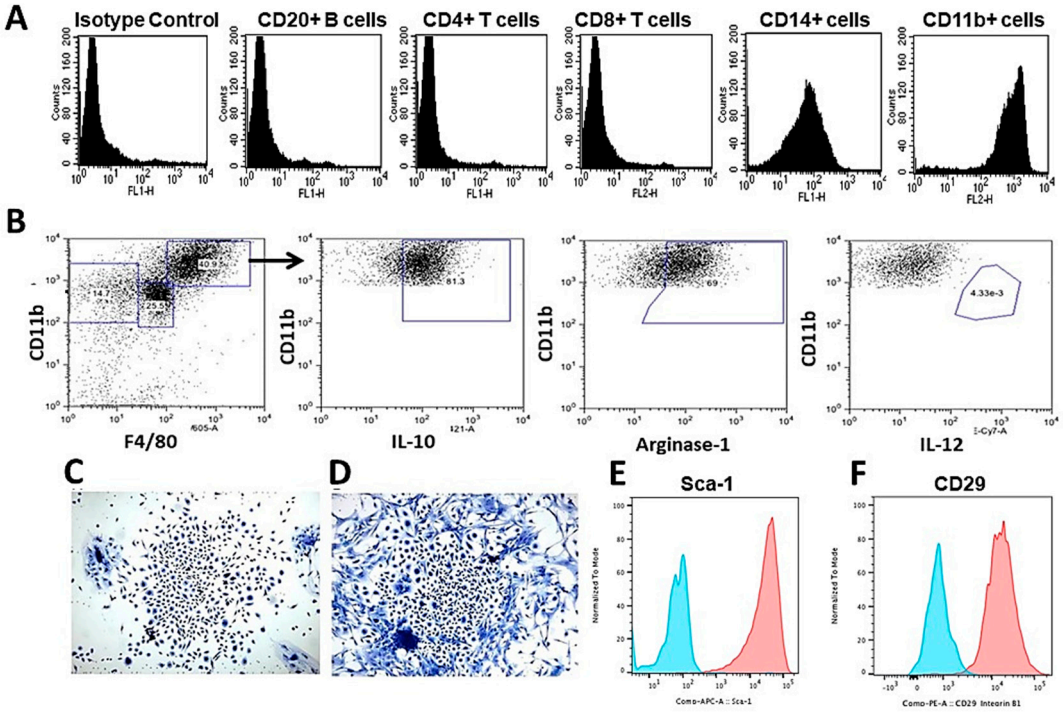

Figure 4. Analysis of cells migrating into PVA sponge discs following anti-Gal/α-gal nanoparticles interaction. A. Flow cytometry analysis of the recruited cells, retrieved from PVA sponge discs containing 10 mg α-gal nanoparticles, 6 days post-subcutaneous implantation. Most of the recruited cells were macrophages expressing CD11b and CD14 cell markers, whereas no significant infiltration of T cells, or B cells was observed (representative data of five mice). B. Analysis of recruited macrophages polarization. The large size macrophages ($CD11b^{pos}/F4/80^{pos}$) were positive also for IL-10 and Arginase-1 but were negative for IL-12. This implied that the majority of the recruited cells were M2 macrophages. C and D. Cell colonies formed by what seemed to be MSC recruited by macrophages migrating into PVA sponge discs containing α-gal nanoparticles and harvested 6 days post subcutaneous implantation. The colonies were observed on Day 5 post culturing. E and F. Expression of MSC markers Sca-1 and CD-29 respectively, by cells harvested from colonies as those in Figure 4C,D. Isotype controls are blue curves. Modified from ref. 58 with permission.

Further analysis of the polarization state of macrophages recruited by a-gal nanoparticles indicated that they were M2 macrophages since they were positively immunostained for M2 markers IL-10 and Arginase-1 and were negatively immunostained for IL-12, a marker which characterizes M1 macrophages (Figure 4B) [57]. When these infiltrating macrophages were cultured *in vitro* for 5 days, the culture wells were found to contain cell colonies at a frequency of one colony per 50,000 to 100,000 cultured macrophages. These cell colonies had the morphological characteristics of colonies formed by MSC (Figure 4C,D). Accordingly, the majority of the cells retrieved from these colonies presented the stem cell markers Sca-1 and CD-29 (Figure 4E,F). These colonies contained 300-1000 cells per colony, suggesting that the cells forming them proliferated at an average cell-cycle time of ~12 hours. Overall, the observations in Figure 4B–F suggest that the majority of macrophages recruited and activated by a-gal nanoparticles polarized into M2 macrophages and further directed migration of MSC into the implanted PVA sponge discs [58].

9. Accelerated Healing of Burns by Topical Application of a-gal Nanoparticles

The above *in vitro* and *in vivo* studies on the effects of a-gal nanoparticles on macrophages (Figures 3 and 4, respectively) prompted the analysis of effects of these nanoparticles on burns healing in anti-Gal producing GT-KO mice [17]. For this purpose, 10 mg a-gal nanoparticles from a suspension containing 100 mg/ml, were dried under sterile conditions on 1x1cm pads of small "spot"

Preprints (www.preprints.org) | NOT PEER-REVIEWED | Posted: 6 September 2023 doi:10.20944/preprints202309.0375.v1

bandages. Pads with dried 0.1ml saline served as controls. Two thermal injuries were performed on shaved two abdominal flanks of anesthetized mice by a brief contact of heated end of a metal spatula (~2x3 mm), resulting in a second degree burn affecting epidermis and dermis, but not the hypodermis. The right side burns were covered with α-gal nanoparticles coated spot bandages, and the left side burns with control saline containing spot bandages (Figure 5A). Removal of the bandages by the mice was prevented by covering them with Tegaderm™ and with Transpore™ adhesive tape. The dressings were removed at various time points, the extent of covering the burn by re-epithelialization and macrophage infiltration were measured and the burn areas were sectioned and subjected to histologic staining by hematoxylin & eosin (H&E) (Figures 5B,C and 6) and by Mason trichrome that stains collagen blue (Figure 7). The extent of macrophages infiltrates into burns and of re-epithelialization (i.e., covering of the burn injury by regenerating epidermis) are presented in Figures 8A and 8B, respectively.

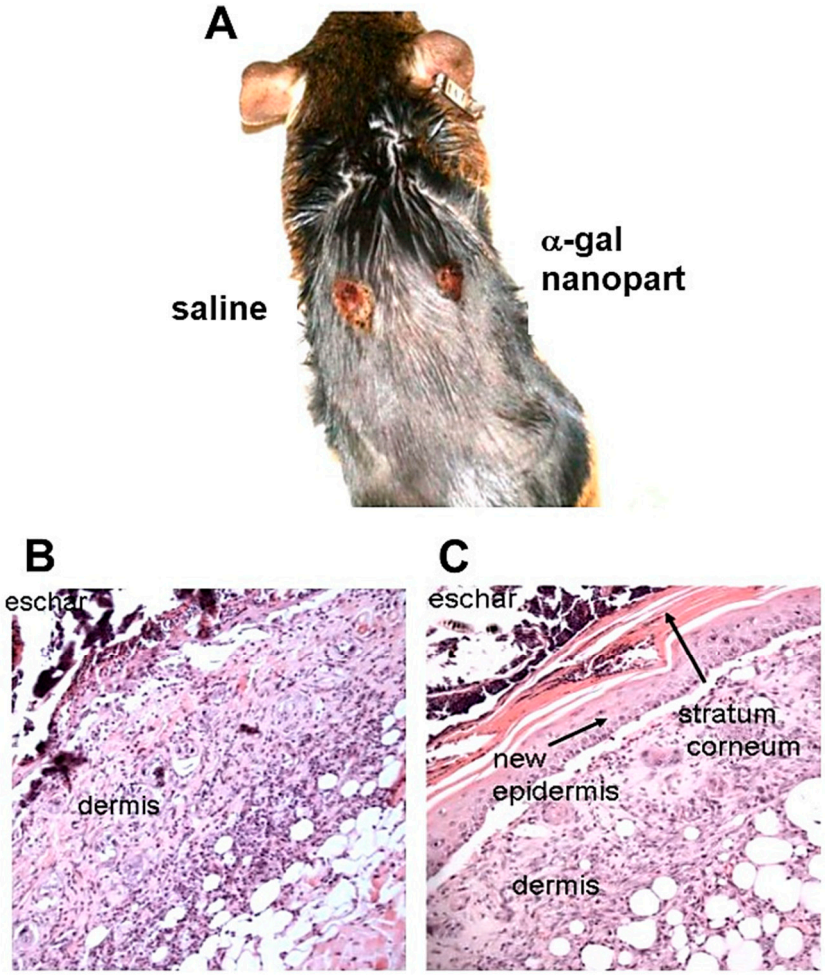

Figure 5. Demonstration of an α-gal nanoparticles treated burn and saline control burn in a representative anti-Gal producing GT-KO mouse, 6 days post thermal injuries and treatment. A. Gross morphology. Note the big difference in the healing of the two burns. B. Histology of the saline treated burn presented in A. No epidermis growth is observed over the dermis which is covered by the eschar. C. Histology of α-gal nanoparticles treated burn presented in A. The burn is covered by the regenerating epidermis including *stratum corneum* and the eschar is observed above the regenerating *stratum corneum*. (H&E, x100). Based on observations in ref. 17.

Preprints (www.preprints.org) | NOT PEER-REVIEWED | Posted: 6 September 2023 doi:10.20944/preprints202309.0375.v1

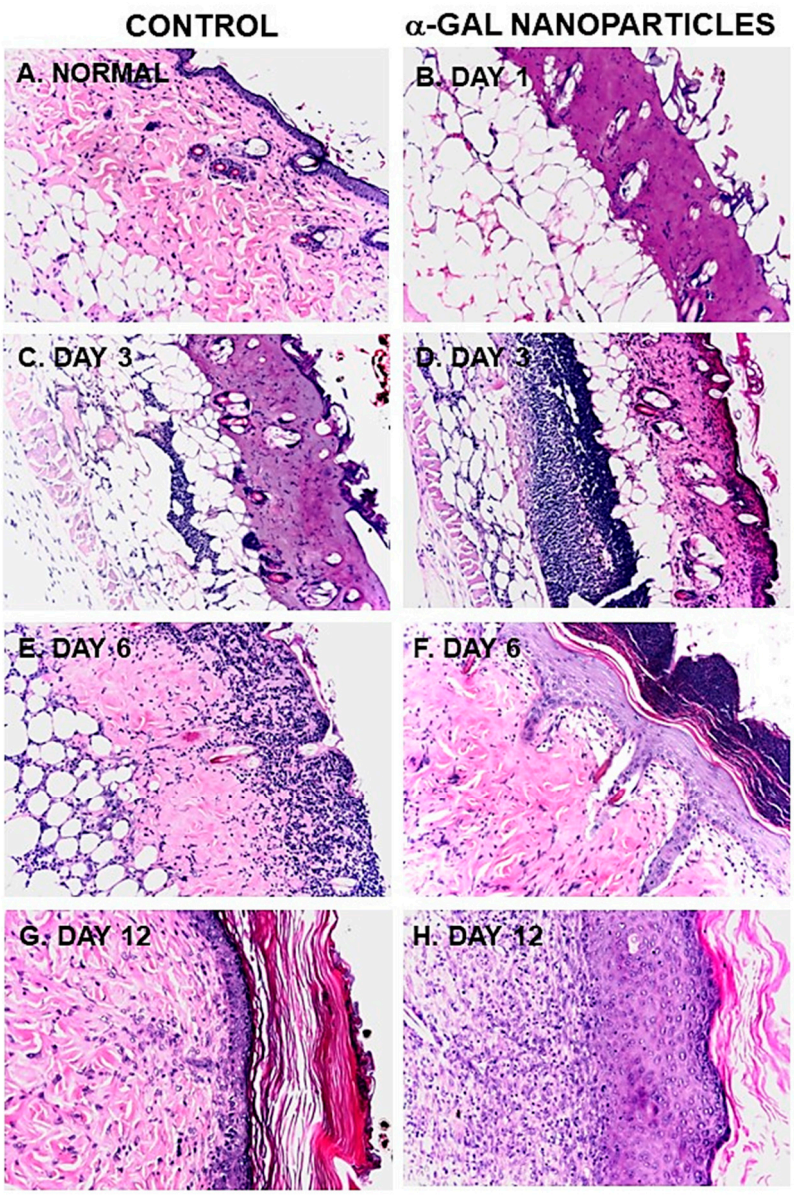

Figure 6. Histology of the accelerated healing of representative burns in anti-Gal producing GT-KO mice treated with α-gal nanoparticles, at various days post treatment. A. Normal mouse skin. B. A burn, 24 hours post injury, displaying histology similar to second-degree burns in humans in that epidermis and dermis are destroyed, but not the hypodermis. C. Saline-treated burn on Day 3. D. α-Gal nanoparticles treated burn on Day 3, characterized by extensive recruitment of macrophages and neutrophils in the injured dermis. E. Saline-treated burn on Day 6 demonstrating migration of macrophages and neutrophils toward the surface of the burn. F. α-Gal nanoparticles treated burn on Day 6 displaying complete regeneration of the epidermis, including *stratum corneum*. Most of the recruited macrophages demonstrated on Day 3 in the dermis are observed on Day 6 above and within the apical part of the *stratum corneum*. G and H. Day 12 demonstrates complete regrowth of the regenerative epidermis in healing burns treated with saline and α-gal nanoparticles, respectively. Specimens are presented in pairs obtained from the same mouse and are representative of five mice at each time point (H&E, x100). Reproduced with permission from ref. 17.

Preprints (www.preprints.org) | NOT PEER-REVIEWED | Posted: 6 September 2023 doi:10.20944/preprints202309.0375.v1

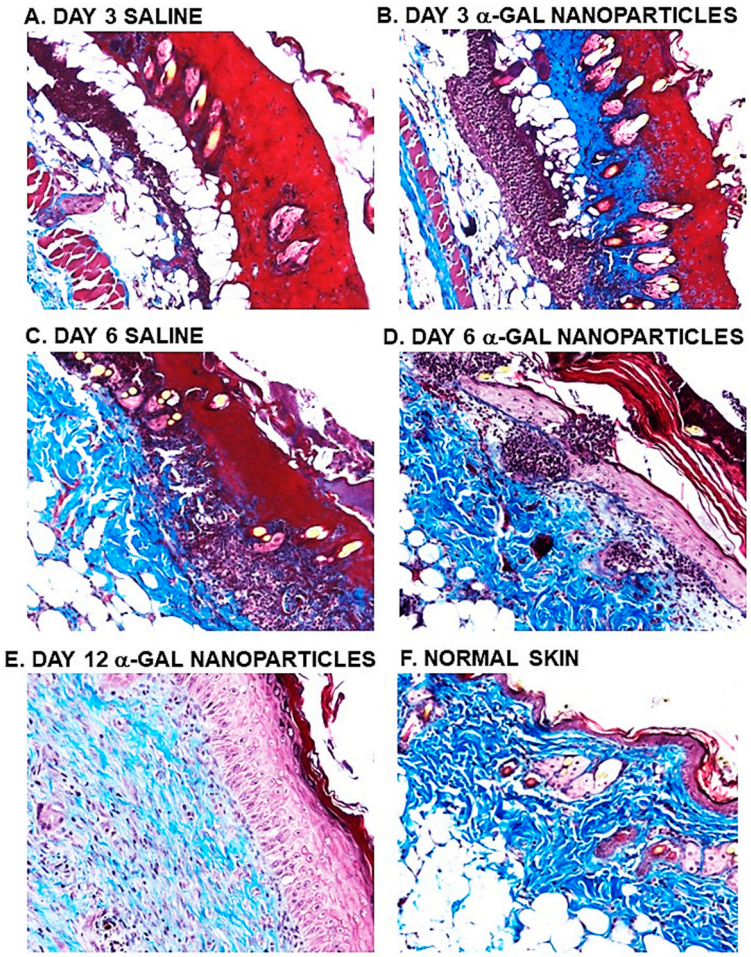

Figure 7. Determination of dermis regeneration as evaluated by Mason trichrome staining blue of *de novo* formed collagen in saline treated (A and C) and in α-gal nanoparticles treated burns (B, D and E). Normal uninjured skin is presented in (F). Specimens A-D are presented in pairs obtained from the same mouse and are representative of five mice at each time point (x100).

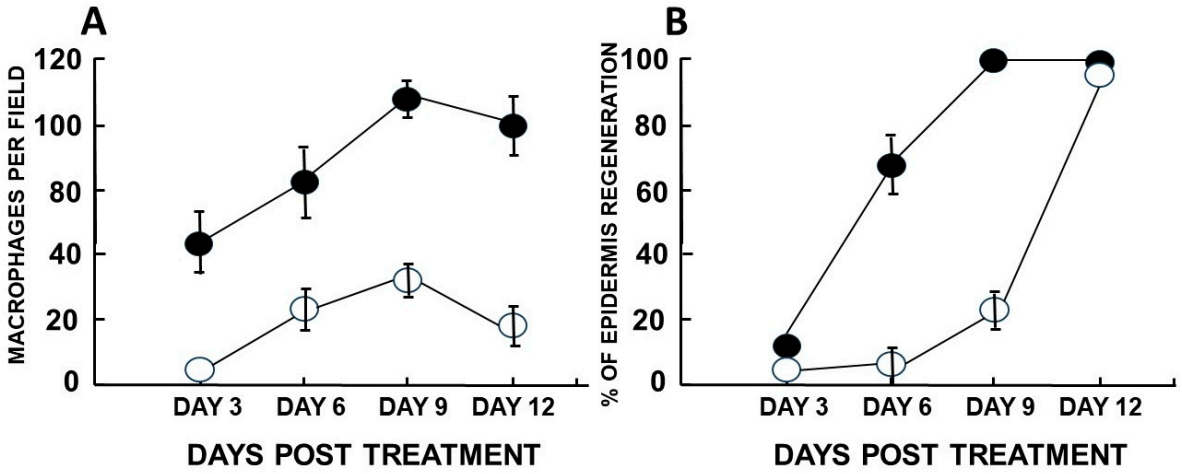

Figure 8. Quantification of macrophage infiltration (A) and burn healing determined by % of epidermal regeneration (B) in burns treated with α-gal nanoparticles or with saline. A. The number of infiltrating macrophages at various time points was determined in histological sections by counting cells within a rectangular area marked in a microscope lens at magnification of x400. B. The proportion (%) of epidermis regeneration was determined histologically by the proportion of the burn surface

 doi:10.20944/preprints202309.0375.v1

covered with the newly formed epidermis. Mean ± S.E. from five mice per group. Adapted based on data in ref. 17.

The histology of a representative normal mouse skin is presented in Figures 6A and 7F. The epidermis in such skins is comprised of 2-3 layers of epithelial cells, the underlying dermis is stained pink by H&E and blue by Mason trichrome and the hypodermis contained mostly fat tissue, characterized by multiple adipocytes. The thermal injuries in the mouse skin resulted in destruction of both the epidermis and the dermis, as observed 24 hours post injury (Figure 6B). This damage is similar to second degree burns in humans, in that both epidermis and dermis are destroyed, whereas damage to the hypodermis is minimal. No differences have been observed 24 hours post injury in a-gal nanoparticles treated burns (Figure 6B) and in burns treated with saline (not shown).

A major difference was observed between treated and control burns, inspected 3 days post injury. Whereas no significant number of macrophages was observed in control burns, as many as 40 macrophages were detected in same size field in a-gal nanoparticles treated burns (Figures 6C,D and 8A). In addition, control burns displayed some degree of neutrophils infiltration, but a-gal nanoparticles treated burns displayed ~5 fold higher number of neutrophils (Figure 6C,D).

The most dramatic difference between the two burn treatments was observed 6 days post thermal injury. At that time point, a-gal nanoparticles treated burns displayed extensive regeneration of epidermis as 50-100% re-epithelialization of the surface areas (mean of ~70%) (Figure 8B). The newly formed epidermis also included formation of *stratum corneum* (Figures 5C and 6D). Many of the macrophages and neutrophils were found to be removed to the surface of the regenerating epidermis, above the *stratum corneum* and were mixed with remnants of the eschar. This accelerated healing was found to be dose depended since 1 mg of a-gal nanoparticles induced an average of 23% healing after 6 days and 0.1 mg elicited not measurable healing [17]. No significant epidermis regeneration was observed on Day 6 in control burns (Figures 5B, 6C and 8B). Nevertheless, the dermis displayed increasing numbers of macrophages in a state of migration to the apical area of the injured dermis.

Evaluation of dermis regeneration was performed by Mason trichrome which stained blue *de novo* synthesized collagen. Near complete regeneration of the dermis was observed in a-gal nanoparticles treated burns after 6 days (Figure 7D), whereas in control burns much of the dermis was stained red, characteristic of thermal damage of the dermis (Figures 7A,C). Initial indication of re-epithelialization of control burns was observed on Day 9, in which ~20% of the burn surfaces were covered by regenerating epidermis (Figure 8B). In contrast, 100% of the a-gal nanoparticles treated burns were healed by that time point. By Day 12, all control burns displayed complete healing as that observed in a-gal nanoparticles treated burns (Figures 6G, 6H, 7E and 8B). All treated and control healed burns did not develop keloids. These findings imply that topical application of a-gal nanoparticles to burns accelerates burns healing and cuts the healing time by ~40%-50%. It is of note that in the absence of anti-Gal (e.g., in wild-type mice), no difference in the healing process was observed between control burns and burns treated with a-gal nanoparticles. Both were similar to the healing of control burns in anti-Gal producing GT-KO mice [17].

10. α-.Gal Nanoparticles Mediated Accelerated Healing of Wounds

Since both healing processes of burns and wounds are mediated by macrophages, it was of interest to determine whether a-gal nanoparticles treatment has similar accelerating effects on wound healing in anti-Gal producing GT-KO mice, as the effects described above in burns healing. Oval shaped full thickness wounds (~6x9 mm) were performed in anesthetized anti-Gal producing GT-KO mice. The wounds were covered with spot bandage dressings containing 10 mg dried a-gal nanoparticles or with control spot bandage dressing containing saline. The healing of the wounds was evaluated by re-epithelialization at various time points. As with treated burns, wounds treated with a-gal nanoparticles completely healed by Day 6 post treatment, whereas control wounds healed only after 12-14 days [18,48]. Studies on completely healed treated and control wounds, 28 days post injury, indicated that, healing of saline treated control wounds resulted in fibrosis and scar formation,

 doi:10.20944/preprints202309.0375.v1

characteristic to the physiologic default healing of untreated wounds. In contrast, healing of a-gal nanoparticles treated wounds resulted in restoration of the normal structure of skin including re-appearance of skin appendages such as hair, sebaceous glands, and hypodermal adipocytes [48]. It was suggested that the accelerated recruitment and activation of macrophages resulted in regeneration of the normal skin structure prior to the initiation of the default fibrosis and scar formation processes, thereby avoiding the latter processes [18,47]. It should be noted that a similar healing that includes restoration of the original structure and function was observed in anti-Gal producing GT-KO mice following myocardial infarction (MI) which was treated by injections of a-gal nanoparticles [59]. In contrast, post infarction ischemic myocardium injected with saline displayed fibrosis and scar formation, similar to the pathology observed in post-MI injured myocardium in humans.

11. Concluding Remarks

Burn healing can be accelerated by the use of a-gal nanoparticles, which harness the immunologic potential of the natural anti-Gal antibody, an abundant antibody in humans constituting ~1% of immunoglobulins. Application of a-gal nanoparticles to burns results in binding of anti-Gal to the a-gal epitopes on these nanoparticles. This interaction activates the complement system, resulting in formation of complement cleavage chemotactic peptides, that direct rapid and extensive migration of monocytes derived macrophages into the treated burns. These recruited macrophages bind via their Fcg receptors the Fcg "tails" of anti-Gal coating the a-gal nanoparticles and are activated to into an M2 polarization state. The activated macrophages further produce a variety of cytokines/growth factors that mediate accelerated regrowth of the epidermis and regeneration of the injured dermis. In anti-Gal producing mice the accelerated epidermal regrowth results in covering of burn with intact epidermis, twice as fast as physiologic regrowth. Similarly, healing of a-gal nanoparticles treated burns in these mice is 40–60% faster than physiologic burn healing. The a-gal nanoparticles are non-toxic, and do not induce chronic granulomas or keloids. In addition, the a-gal nanoparticles are highly stable for long periods at various temperatures, and in view of their accelerated healing effects they may be considered for treatment of human burns. Accelerated healing by a-gal nanoparticles is also observed in treated wounds of anti-Gal producing mice. Application of a-gal nanoparticles to burns and wounds may be feasible in the form of dried nanoparticles on wound dressings and as suspensions, aerosols, hydrogels, or incorporated into sheets of biodegradable scaffold materials such as collagen sheets.

References

1. Mahdavian Delavary, B.; van der Veer, W M.; van Egmond, M.; Niessen, F.B.; Beelen, R.H. Macrophages in skin injury and repair. Immunobiology. 2011, 216, 753–762.
2. DiPietro, L.A.; Koh, T.J. Macrophages and wound healing. Adv. Wound Care 2016, 2, 71–75.
3. Suda, S.; Williams, H.; Medbury, H.J.; Holland. A.J. A Review of Monocytes and Monocyte-Derived Cells in Hypertrophic Scarring Post Burn. J. Burn Care Res. 2016, 37, 265 72.
4. Penatzer JA, Srinivas S, Thakkar RK. The role of macrophages in thermal injury. Int J Burns Trauma. 2022 Feb 15;12(1):1-12.
5. Italiani, P.; Boraschi, D. From Monocytes to M1/M2 macrophages: phenotypical vs. functional differentiation. Front. Immunol. 2014, 5, 514.
6. Singer, A.J; Clark, R.A. Cutaneous wound healing. N. Engl. J. Med. 1999, 341,738–746.
7. Jeschke, M.G.; van Baar, M.E.; Choudhry, M.A.; Chung, K.K.; Gibran, N.S.; Logsetty, S. Burn injury. Nat. Rev. Dis. Primer. 2020, 6, 11
8. Piccolo, M.T.; Wang, Y.; Sannomiya, P.; Piccolo, N.S.; Piccolo, M.S.; Hugli, T.E.; Ward, P.A.; Till, G.O. Chemotactic mediator requirements in lung injury following skin burns in rats. Exp. Mol. Pathol. 1999, 66, 220–226.
9. Shukaliak, J.; Dorovini-Zis, K. Expression of the [β]-Chemokines RANTES and MIP-1β by Human Brain Microvessel Endothelial Cells in Primary Culture. J. Neuropathol. Exp. Neurol. 2000, 59, 339–352.

10. Shallo, H.; Plackett, T.P.; Heinrich, S.A.; Kovacs, E.J. Monocyte chemoattractant protein-1 (MCP-1) and macrophage infiltration into the skin after burn injury in aged mice. Burns 2003, 29, 641–647.
11. Heinrich, S.A.; Messingham, K.A.; Gregory, M.S.; Colantoni, A.; Ferreira, A.M.; Dipietro, L.A.; Kovacs, E.J. Elevated monocyte chemoattractant protein-1 levels following thermal injury precede monocyte recruitment to the wound site and are controlled, in part, by tumor necrosis factor-α. Wound Repair Regen. 2003, 11, 110–119.
12. Tyler MP, Watts AM, Perry ME, Roberts AH, McGrouther DA. Dermal cellular inflammation in burns. An insight into the function of dermal microvascular anatomy. Burns 2001, 27, 433-438.
13. Martin, P.; Leibovich, S. J. Inflammatory cells during wound repair: the good, the bad and the ugly. Trends . Biol. 2005, 15, 599–607.
14. Franz, M.G.; Steed, D.L.; Robson, M.C. Optimizing healing of the acute wound by minimizing complications. Curr. Probl. Surg. 2007, 4, 691–763.
15. Alexander, M.; Chaudry, I.H.; Schwacha, M.G. Relationships between burn size, immunosuppression, and macrophage hyperactivity in a murine model of thermal injury. Cell. Immunol. 2002, 220, 63–69.
16. Schwacha, M.G. Macrophages and post-burn immune dysfunction. Burns 2003, 29, 1–14.
17. Galili, U.; Wigglesworth, K.; Abdel-Motal, U.M. Accelerated healing of skin burns by anti-Gal/α-gal liposomes interaction. Burns 2010, 36, 239–251.
18. Galili, U. α-Gal Nanoparticles in Wound and Burn Healing Acceleration. Adv. Wound Care (New Rochelle). 2017, 6, 81–92.
19. Hocking, A.M. Mesenchymal Stem Cell Therapy for Cutaneous Wounds. Adv. Wound Care (New Rochelle). 2012 1, 166-171.
20. Jo, H., Brito, S.; Kwak, B.M.; Park, S.; Lee, M.G.; Bin, B.H. Applications of Mesenchymal Stem Cells in Skin Regeneration and Rejuvenation. Int. J. Mol. Sci. 2021, 22, 2410.
21. Hernon, C,A.; Dawson, R.A.; Freedlander, E.; Short, R.; Haddow, D.B.; Brotherston, M.; MacNeil, S. Clinical experience using cultured epithelial autografts leads to an alternative methodology for transferring skin cells from the laboratory to the patient. Regen. Med. 2006 1, 809–821.
22. Lee, H. Outcomes of sprayed cultured epithelial autografts for full-thickness wounds: a single-centre experience. Burns 2012, 38, 931–936.
23. Yuan, L.; Minghua, C.; Feifei, D.; Runxiu, W.; Ziqiang, L.; Chengyue, M., Wenbo, J. Study of the use of recombinant human granulocyte-macrophage colony-stimulating factor hydrogel externally to treat residual wounds of extensive deep partial-thickness burn. Burns 2015, 41, 1086–1091.
24. Yan, D.; Liu, S.; Zhao, X.; Bian, H.; Yao. X.; Xing, J.; Sun, W.; Chen, X. Recombinant human granulocyte macrophage colony stimulating factor in deep second-degree burn wound healing. Medicine (Baltimore) 2017, 96, e6881.
25. Lavker, R.M.; Kaplan, N.; McMahon, K.M.; Calvert, A.E.; Henrich, S.E.; Onay, U.V.; Lu, K.Q.; Peng, H.; Thaxton, C.S. Synthetic high-density lipoprotein nanoparticles: Good things in small packages. Ocul. Surf. 2021, 21,19-26.
26. Hermosilla, J.; Pastene-Navarrete, E.; Acevedo, F. Electrospun Fibers Loaded with Natural Bioactive Compounds as a Biomedical System for Skin Burn Treatment. A Review. Pharmaceutics 2021,13, 2054;
27. Weng, T.; Wang, J.; Yang, M.; Zhang, W.; Wu, P.; You, C.; Han, C.; Wang, X. Nanomaterials for the delivery of bioactive factors to enhance angiogenesis of dermal substitutes during wound healing. Burns Trauma 2022, 10, tkab049.
28. Frear, C.C.; Griffin, B.R.; Cuttle, L.; Kimble, R.M.; McPhail, S.M. Cost-effectiveness of adjunctive negative pressure wound therapy in pediatric burn care: evidence from the SONATA in C randomized controlled trial. Sci. Rep. 2021, 11, 16650.
29. Galili, U.; Rachmilewitz, E.A.; Peleg, A.; Flechner, I. A unique natural human IgG antibody with anti-α-galactosyl specificity. J. Exp. Med. 1984, 160, 1519–1531.
30. Galili, U.; Mandrell, R.E.; Hamadeh, R.M.; Shohet, S.B.; Griffiss, J.M. Interaction between human natural anti-α-galactosyl immunoglobulin G and bacteria of the human flora. Infect. Immun. 1988, 56, 1730–1737.
31. Mañez, R.; Blanco, F.J.; Díaz, I.; Centeno, A.; Lopez-Pelaez, E.; Hermida, M.; Davies, H.F.; Katopodis, A. Removal of bowel aerobic gram-negative bacteria is more effective than immunosuppression with cyclophosphamide and steroids to decrease natural α-galactosyl IgG antibodies. Xenotransplantation 2001, 8, 15–23.

32. Galili, U.; Macher, B.A.; Buehler, J.; Shohet, S.B. Human natural anti-α-galactosyl IgG. II. The specific recognition of α[1,3]-linked galactose residues. J. Exp. Med. 1985, 162, 573–582.
33. Towbin, H.; Rosenfelder, G.; Wieslander, J.; Avila, J.L.; Rojas, M.; Szarfman, A.; Esser, K.; Nowack, H.; Timpl, R. Circulating antibodies to mouse laminin in Chagas disease, American cutaneous leishmaniasis, and normal individuals recognize terminal galactosyl [α1-3]-galactose epitopes. J. Exp. Med. 1987, 166, 419–432.
34. Teneberg, S.; Lönnroth, I.; Torres Lopez, J.F.; Galili, U.; Olwegard Halvarsson, M.; Angstrom, J.; Karlsson, K.A. Molecular mimicry in the recognition of glycosphingolipids by Galα3Galß4GlcNAcß-binding Clostridium difficile toxin A, human natural anti-α-galactosyl IgG and the monoclonal antibody Gal-13: Characterization of a binding-active human glycosphingolipid, non-identical with the animal receptor. Glycobiology 1996, 6, 599–609.
35. Galili, U.; Clark, M.R.; Shohet, S.B.; Buehler, J.; Macher, B.A. Evolutionary relationship between the anti-Gal antibody and the Galα1-3Gal epitope in primates. Proc. Natl. Acad. Sci. USA 1987, 84, 1369–1373.
36. Galili, U.; Shohet, S.B.; Kobrin, E.; Stults, C.L.M.; Macher, B.A. Man, apes, and Old-World monkeys differ from other mammals in the expression of α-galactosyl epitopes on nucleated cells. J. Biol. Chem. 1988, 263, 17755–17762.
37. Thall, A.; Galili, U. Distribution of Gal alpha 1----3Gal beta 1----4GlcNAc residues on secreted mammalian glycoproteins (thyroglobulin, fibrinogen, and immunoglobulin G) as measured by a sensitive solid-phase radioimmunoassay. Biochemistry 1990, 29, 3959–3965.
38. Oriol, R.; Candelier, J.J.; Taniguchi, S.; Balanzino, L.; Peters, L.; Niekrasz, M.; Hammer, C.; Cooper, D.K. Major carbohydrate epitopes in tissues of domestic and African wild animals of potential interest for xenotransplantation research. Xenotransplantation 1999, 6, 79–89.
39. Cooper, D.K.C.; Good, A.H.; Koren, E.; Oriol, R.; Malcolm, A.J.; Ippolito, R.M.; Neethling, F.A.; Ye, Y.; Romano, E.; Zuhdi, N. Identification of α-galactosyl and other carbohydrate epitopes that are bound by human anti-pig antibodies: Relevance to discordant xenografting in man. Transpl. Immunol. 1993, 1, 198–205.
40. Galili, U. Interaction of the natural anti-Gal antibody with α-galactosyl epitopes: A major obstacle for xenotransplantation in humans. Immunol. Today 1993, 14, 480–482
41. Sandrin, M.S.; Vaughan, H.A.; Dabkowski, P.L.; McKenzie, I.F.C. Anti-pig IgM antibodies in human serum react predominantly with Gal (αl-3)Gal epitopes. Proc. Natl. Acad. Sci. USA 1993, 90, 11391–11395.
42. Collins, B.H.; Cotterell, A.H.; McCurry, K.R.; Alvarado, C.G.; Magee, J.C.; Parker, W.; Platt, J.L. Cardiac xenografts between primate species provide evidence for the importance of the α-galactosyl. determinant in hyperacute rejection. J. Immunol. 1995, 154, 5500–5510.
43. Repik, P.M.; Strizki, M.; Galili, U. Differential host dependent expression of α-galactosyl epitopes on viral glycoproteins: A study of Eastern equine encephalitis virus as a model. J. Gen. Virol. 1994, 75, 1177–1181.
44. Pipperger, L.; Koske, I.; Wild, N.; Müllauer, B.; Krenn, D.; Stoiber, H.; Wollmann, G.; Kimpel, J.; von Laer, D.; Bánki, Z. Xenoantigen-dependent complement-mediated neutralization of LCMV glycoprotein pseudotyped VSV in human serum. J. Virol. 2019, 93, e00567-19.
45. Takeuchi, Y.; Porter, C.D.; Strahan, K.M.; Preece, A.F.; Gustafsson, K.; Cosset, F.L.; Weiss, R.A.; Collins, M.K. Sensitization of cells and retroviruses to human serum by [α1-3] galactosyltransferase. Nature 1996, 379, 85–88.
46. Preece, A.F.; Strahan, K.M.; Devitt, J.; Yamamoto, F.; Gustafsson, K. Expression of ABO or related antigenic carbohydrates on viral envelopes leads to neutralization in the presence of serum containing specific natural antibodies and complement. Blood 2002, 99, 2477–2482.
47. Galili, U. book "The natural anti-Gal antibody as foe turned friend in medicine" Academic Press/Elsevier, London, New York, 2018, pp. 207-228.
48. Wigglesworth, K.M.; Racki, W.J.; Mishra, R.; Szomolanyi-Tsuda, E.; Greiner, D.L.; Galili. U. Rapid recruitment and activation of macrophages by anti-Gal/α-Gal liposome interaction accelerates wound healing. J. Immunol. 2011, 186, 4422-4432.
49. Thall, A.D.; Maly, P.; Lowe, J.B. Oocyte Gal 1,3Gal epitopes implicated in sperm adhesion to the zona pellucida glycoprotein ZP3 are not required for fertilization in the mouse. J. Biol. Chem. 1995, 270, 21437-21440.

50. Tearle, R.G.; Tange, M.J.; Zanettino, Z.L.; Katerelos, M.; Shinkel, T.A.; Van Denderen, B.J.; Lonie, A.J.; Lyonsm, I., Nottle, M.B.; Cox, T. et al. The alpha-1,3-galactosyltransferase knockout mouse. Implications for xenotransplantation. Transplantation 1996, 61, 13-19.
51. Lai, L.; Kolber-Simonds, D.; Park, K.W.; Cheong, H.T.; Greenstein, J.L.; Im, G.S.; Samuel, M.; Bonk, A.; Rieke, A.; Day, B.N.; et al. Production of α-1,3-galactosyltransferase knockout pigs by nuclear transfer cloning. Science 2002, 295, 1089–1092.
52. Phelps, C.J.; Koike, C.; Vaught, T.D.; Boone, J.; Wells, K.D.; Chen, S.H.; Ball, S.; Specht, S.M.; Polejaeva, I.A.; Monahan, J.A.; et al. Production of α1,3-galactosyltransferase-deficient pigs. Science 2003, 299, 411–414.
53. Dor, F.J.; Tseng, Y.L.; Cheng, J.; Moran, K.; Sanderson, T.M.; Lancos, C.J.; Shimizu, A.; Yamada, K.; Awwad, M.; Sachs, D.H.; et al. α1,3-Galactosyltransferase gene-knockout miniature swine produce natural cytotoxic anti-Gal antibodies. Transplantation 2004, 78, 15–20.
54. Fang, J.; Walters, A.; Hara, H.; Long, C.; Yeh, P.; Ayares, D.; Cooper, D.K.; Bianchi, J. Anti-gal antibodies in α1,3- galactosyltransferase gene knockout pigs. Xenotransplantation 2012, 19, 305–310.
55. Galili, U. The natural anti-Gal antibody and simulate the evolutionary appearance of this antibody in primates. Xenotransplantation 2013, 20, 267–276
56. Tanemura, M.; Yin, D.; Chong, A.S.; Galili, U. Differential immune responses to α-gal epitopes on xenografts and allografts: Implications for accommodation in xenotransplantation. J. Clin. Investig. 2000, 105, 301–310.
57. Kaymakcalan, O.E.; Abadeer, A.; Goldufsky, J.W.; Galili, U.; Karinja, S.J.; Dong, X.; Jin, J.L.; Samadi, A.; Spector, J.A. Topical α-gal nanoparticles accelerate diabetic wound healing. Exp. Dermatol. 2020, 29, 404–413.
58. Galili, U.; Goldufsky, J.W.; Schaer, G.L. α-Gal Nanoparticles Mediated Homing of Endogenous Stem Cells for Repair and Regeneration of External and Internal Injuries by Localized Complement Activation and Macrophage Recruitment. Int. J. Mol. Sci. 2022, 23, 11490.
59. Galili, U.; Zhu, Z.; Chen, J.; Goldufsky, J.W.; Schaer, G.L. Near Complete Repair After Myocardial Infarction in Adult Mice by Altering the Inflammatory Response With Intramyocardial Injection of α-Gal Nanoparticles. Frontiers Cardiovasc. Med. 2021, 8, 719160.